

acidic lipids.<sup>11</sup> The latter phenomenon plays important roles in regulation of physiological functions such as membrane fusion and secretion.

The interaction of metal ions with the surface ligand of aqueous micelles and bilayers has been studied by several groups. Le Moigne et al.<sup>12,13</sup> reported enhanced interactions of some metal ions with micellar ligands (crown ether and polyamine) and Grätzel et al.<sup>14,15</sup> described acceleration of photoreduction of Ag<sup>+</sup> in related micellar and bilayer systems. Fromherz and Arden<sup>16</sup> examined pH modulation of energy and electron transfer across the bilayer of docosylamine deposited on the electrode surface.

The characteristics of the present membrane system as a signal receptor are summarized as follows. Chemical signals (H<sup>+</sup>, Cu<sup>2+</sup>, and SO<sub>4</sub><sup>2-</sup>) interact specifically with the ethylenediamine moiety (receptor) at the membrane surface, and these specific signals are transduced into nonspecific spectral information via the change in the membrane physical state. The signals can be amplified during this process, since the molecular extinction coefficient of the azobenzene chromophore (23 000) is much larger than, for instance, that of the ethylenediamine Cu<sup>2+</sup> chelate (ca. 50).

The signal recognition can be readily improved by the introduction of other specific ligands at the membrane surface and by the use of more sensitive spectroscopic methods. Efforts directed toward this goal are under way.

**Acknowledgment.** We are grateful for the capable technical assistance of K. Iida and R. Ando.

**Registry No. 1,** 75056-19-8; **2,** 80737-49-1; **3,** 80721-48-8; **4,** 70755-47-4; **5,** 65316-86-1; CuSO<sub>4</sub>, 18939-61-2.

- (11) Ohnishi, S.; Ito, T. *Biochemistry*, **1974**, *13*, 881-887.  
 (12) Le Moigne, J.; Simon, J. *J. Phys. Chem.* **1980**, *84*, 170-177.  
 (13) Simon, J.; Le Moigne, J.; Markovitsi, D.; Dayantis, J. *J. Am. Chem. Soc.* **1981**, *102*, 7247-7252.  
 (14) Monserrat, K.; Grätzel, M.; Tundo, P. *J. Am. Chem. Soc.* **1980**, *102*, 5527-5529.  
 (15) Humphry-Baker, R.; Moroi, Y.; Grätzel, M.; Pelizzetti, E.; Tundo, P. *J. Am. Chem. Soc.* **1980**, *102*, 3689-3692.  
 (16) Fromherz, P.; Arden, W. *J. Am. Chem. Soc.* **1980**, *102*, 6211-6218.

## Strategy for Nitrogen NMR of Biopolymers

T. A. Cross, J. A. DiVerdi, and S. J. Opella\*

*Department of Chemistry, University of Pennsylvania  
 Philadelphia, Pennsylvania 19104*

*Received November 5, 1981*

High-resolution nitrogen NMR spectra of biopolymers are readily obtained by using solid-state <sup>15</sup>N NMR techniques on immobile samples, whether crystalline or slowly reorienting solutions, where the molecules have been highly enriched biosynthetically with <sup>15</sup>N. Nitrogen NMR spectroscopy is very attractive for biophysical studies because there are relatively few nitrogen atoms in biopolymers (compared to carbon or hydrogen) and they are often located in interesting sites such as functionally active residues of enzymes, the bases of DNA and RNA, or the polypeptide backbone of proteins.

The nuclear properties of the stable isotopes of nitrogen present difficulties for high-resolution NMR spectroscopy. <sup>14</sup>N has spin  $S = 1$  with a large quadrupole coupling constant in most situations; as a consequence the powder patterns in solids and the resonances in solution are broad. Recent <sup>14</sup>N solid-state NMR experiments on single crystals<sup>1</sup> and samples with substantial motional averaging<sup>2,3</sup> show considerable promise for these specialized cases. The

- (1) Stark, R. E.; Haberkorn, R. A.; Griffin, R. G. *J. Chem. Phys.* **1978**, *68*, 1996-1999.  
 (2) Siminovitch, D. J.; Rance, M.; Jeffrey, K. R. *FEBS Lett.* **1980**, *112*, 79-82.  
 (3) Rothgeb, T. M.; Oldfield, E. *J. Biol. Chem.* **1981**, *256*, 6004-6009.

other stable isotope of nitrogen is <sup>15</sup>N, which has spin  $S = 1/2$ , but its natural abundance of only 0.3% results in very low sensitivity, and its small, negative gyromagnetic ratio makes even labeled site studies difficult because of long  $T_1$ 's and negative nuclear Overhauser enhancements. Spin  $S = 1/2$  nuclei offer great opportunities for biological NMR spectroscopy because the observation of resonances from individual sites of biopolymers allows measurements that can give structural and dynamical information with atomic resolution. Of the four spin  $S = 1/2$  nuclei found in biopolymers (<sup>1</sup>H, <sup>13</sup>C, <sup>15</sup>N, <sup>31</sup>P) only <sup>15</sup>N has not been widely used in spectroscopic studies. Natural abundance <sup>15</sup>N spectra of biopolymers have single-site resolution only when very concentrated large samples are extensively signal averaged in a high-field spectrometer.<sup>4,5</sup>

There are several advantages to solid-state <sup>15</sup>N NMR experiments. The sensitivity due to cross polarization of the <sup>15</sup>N magnetization from the protons is increased over that from <sup>15</sup>N sampling pulses because of the larger amount of <sup>15</sup>N magnetization developed per transient and the ability to recycle the experiment according to the generally short <sup>1</sup>H  $T_1$ 's rather than the long <sup>15</sup>N  $T_1$ 's.<sup>6</sup> The observed nuclear Overhauser enhancement varies with reorientation rates in solution and can completely eliminate signals in spectra of biopolymers, but is avoided in the cross-polarization experiment. Proton decoupling removes the heteronuclear dipolar interactions, making the <sup>15</sup>N chemical shift properties available for study.<sup>7,8</sup> Magic-angle sample spinning<sup>9</sup> averages the <sup>15</sup>N chemical shift powder patterns to isotropic resonances, with line widths (<0.5 ppm) for polycrystalline amino acids similar to those observed in <sup>13</sup>C NMR spectroscopy.<sup>10</sup>

Meselson and Stahl<sup>11</sup> demonstrated that when *E. coli* are grown on a medium with <sup>15</sup>NH<sub>4</sub>Cl as the sole nitrogen source, <sup>15</sup>N is incorporated into the newly synthesized biopolymers. From growth of *E. coli* with the appropriate genetic makeup,<sup>12</sup> whether wild type or arranged through mutation, cloning, or viral infection, any gene or gene product of procaryotic or eucaryotic origin can be obtained uniformly labeled with <sup>15</sup>N. Very high enrichment with <sup>15</sup>N is advantageous from an NMR point of view because of the increased sensitivity due to the large number of spins without the penalty associated with homonuclear couplings, as seen with uniform <sup>13</sup>C enrichment, since no nitrogens in biopolymers are directly bonded to other nitrogens. Growth on <sup>15</sup>N-containing media has been used to provide several in vivo systems<sup>13-17</sup> and isolated biomolecules,<sup>18-20</sup> including DNA from *E. coli*,<sup>21,22d</sup> for

- (4) Gust, D.; Moon, R. B.; Roberts, J. D. *Proc. Natl. Acad. Sci. U.S.A.* **1975**, *72*, 4696-4700.  
 (5) Hull, W. E.; Bullesbach, E.; Wieneke, H.-J.; Zahn, H.; Kricheldorf, H. R. *Org. Magn. Reson.* **1981**, *17*, 92.  
 (6) Pines, A.; Gibby, M. G.; Waugh, J. S. *J. Chem. Phys.* **1973**, *59*, 569-590.  
 (7) Gibby, M.; Griffin, R. G.; Pines, A.; Waugh, J. S. *Chem. Phys. Lett.* **1972**, *17*, 80-81.  
 (8) Harbison, G.; Herzfeld, J.; Griffin, R. G. *J. Am. Chem. Soc.* **1981**, *103*, 4752-4754.  
 (9) Andrew, E. R.; Bradbury, A.; Eades, R. G. *Nature (London)* **1958**, *182*, 1659.  
 (10) Opella, S. J.; Hexem, J. G.; Frey, M. H.; Cross, T. A. *Phil. Trans. R. Soc. London Ser. A* **1981**, *299*, 665-683.  
 (11) Meselson, M.; Stahl, F. W. *Proc. Natl. Acad. Sci. U.S.A.* **1958**, *44*, 671-682.  
 (12) Wu, R., Ed. *Methods Enzymol.* **1979**, *68*, 1-555.  
 (13) Llinas, M.; Wuthrich, K.; Schwatzer, W.; von Philipsborn, W. *Nature (London)* **1975**, *257*, 817-818.  
 (14) Lapidot, A.; Irving, C. S. *Proc. Natl. Acad. Sci. U.S.A.* **1977**, *74*, 1988-1992.  
 (15) Schaefer, J.; Stejskal, E. O.; McKay, R. A. *Biochem. Biophys. Res. Commun.* **1979**, *88*, 274-280.  
 (16) Jacob, G. C.; Schaefer, J.; Stejskal, E. O.; McKay, R. A. *Biochem. Biophys. Res. Commun.* **1980**, *97*, 1176-1182.  
 (17) Legerton, T. L.; Kanamori, K.; Weiss, R. L.; Roberts, J. D. *Proc. Natl. Acad. Sci. U.S.A.* **1981**, *78*, 1495-1498.  
 (18) (a) Llinas, M.; Horsley, W. J.; Klein, M. P. *J. Am. Chem. Soc.* **1976**, *98*, 632-634. (b) Llinas, M.; Wuthrich, K. *Biochim. Biophys. Acta* **1978**, *532*, 29-40.  
 (19) (a) Lapidot, A.; Irving, C. S.; Malik, Z. *J. Am. Chem. Soc.* **1976**, *98*, 632-634. (b) Lapidot, A.; Irving, C. S. *Ibid.* **1977**, *99*, 5488-5490.  
 (20) Bachovchin, W. W.; Roberts, J. D. *J. Am. Chem. Soc.* **1978**, *100*, 8041-8047.

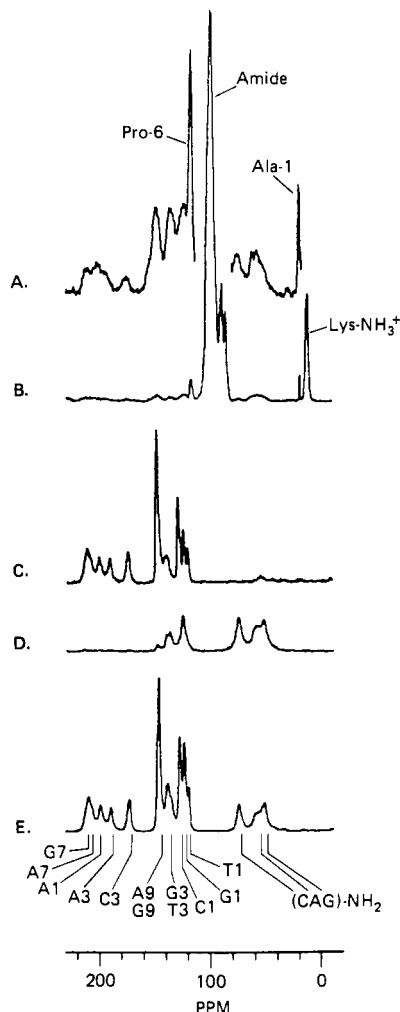


**Figure 1.**  $^{15}\text{N}$  NMR spectra of B-DNA and fd virus. The spectra were obtained at a resonance frequency of 15.24 MHz on a home-built double-resonance spectrometer with the spin-lock method of cross polarization using mix times as listed with proton decoupling (1.5 mT) during data acquisition (50 ms). The samples packed in Andrew-Beams rotors were spinning (2.2 kHz) at the magic angle ( $55^\circ$ ) with respect to the applied magnetic field. Chemical shifts are referenced to external  $^{15}\text{NH}_4\text{NO}_3$ . (A) Vertical expansion of B. (B) Complete  $^{15}\text{N}$  NMR spectrum of fd with 2-ms mix time for 6000 transients. Spinning sidebands were suppressed by using the technique described by Dixon.<sup>35</sup> (C) Nonprotonated  $^{15}\text{N}$  NMR spectrum of B-DNA with 4-ms mix time for 1000 transients. Resonances from proton-bearing nitrogens were suppressed by using the technique described by Opella and Frey.<sup>21</sup> (D) Protonated  $^{15}\text{N}$  NMR spectrum of B-DNA with 0.05-ms mix time for 1000 transients. Resonances from non-proton-bearing nitrogens were suppressed by virtue of the short mix time. (E) Complete  $^{15}\text{N}$  NMR spectrum of B-DNA with 4-ms mix time for 4000 transients. (F) Identification of  $^{15}\text{N}$  resonance line positions in ppm: G7, 211.1; A7, 208.5; A1, 200.3; A3, 190.8; C3, 174.1; A9, 147.5; G9, 147.5; G3, 139.6; T3, 136.1; C1, 128.9; G1, 124.4; T1, 120.6; C-NH<sub>2</sub>, 75.7; A-NH<sub>2</sub>, 59.3; G-NH<sub>2</sub>, 52.7.

NMR studies. The samples used here were obtained from *E. coli* infected with the filamentous bacteriophage fd and grown on a minimal, chemically defined medium with  $^{15}\text{NH}_4\text{Cl}$  as the sole nitrogen source. The duplex DNA from the cells and the virus

from the growth medium were isolated and purified by standard methods;<sup>23,24</sup> the NMR samples were prepared by hydrating the ethanol-precipitated DNA and by pelleting fd in an ultracentrifuge.

The complete  $^{15}\text{N}$  NMR spectrum of solid B form DNA is shown in Figure 1E. Figures 1C and 1D demonstrate that excellent selectivity between proton-bearing and non-proton-bearing nitrogen sites is possible by relying on the relative strengths of the  $^1\text{H}$ - $^{15}\text{N}$  dipolar couplings.<sup>25</sup> Resolved resonances for 13 of the 14 nitrogen sites of DNA are observed in Figure 1C-E despite the relatively low resonance frequency (15.24 MHz). The DNA resonances are generally broader (2–6 ppm) than those of the corresponding crystalline small molecules because of the dispersive effects of sequence and conformational heterogeneity. Many of the DNA resonance frequencies are within 1–2 ppm of the values observed for nucleosides or nucleotides in solution. Inter- or intrastrand neighbor effects are evident in the thymine N1 resonance, which is split into two lines (120–121 ppm) in Figure 1C, and the apparent 4–16 ppm upfield shifts of some resonances, including the C3 and A1 nitrogens, which are hydrogen-bond acceptors.<sup>26</sup>

The bacteriophage fd consists almost entirely of 2700 copies of the major coat protein (90%) and a single stranded circle of DNA (10%).  $^{15}\text{N}$  NMR spectroscopy offers the possibility of simultaneously studying the DNA and protein components of the virus, since there is little overlap among the chemical shifts of the constituents of these biopolymers.<sup>22,27–29</sup> The  $^{15}\text{N}$  NMR spectrum of fd in Figure 1B shows the narrow, high-intensity protein resonances well separated from the broad, low-intensity DNA resonances. The protein spectrum is dominated by the intense amide resonance band (98.5 ppm), with lines from the glutamine side chain and the glycines at 85–90 ppm. The five lysine  $\epsilon$ -amino groups give the resonance at 12 ppm. Of particular interest are the resolved resonances from the single proline residue (Pro-6, 117 ppm) and the amino terminal alanine residue (Ala-1; 19 ppm) of the coat protein, which demonstrate that single atomic site resolution is possible with this strategy for  $^{15}\text{N}$  NMR of proteins.<sup>30</sup> The individual Pro-6 and Ala-1 resonances, as well as the viral DNA resonances, are clearly visible in the expanded spectrum of Figure 1A. The single stranded circular DNA packed inside the viral coat has nitrogen resonance bands that differ in shape and relative intensities from those of duplex DNA seen by comparison of Figures 1 parts A and E; these spectral changes in DNA resonances can be accounted for with shifts on the order of 1–5 ppm due to the influence of the coat proteins on the DNA.

The availability of well-resolved  $^{15}\text{N}$  isotropic chemical shift spectra of biopolymers offers many possibilities for informative NMR experiments. Structural information is available from the precise chemical shift frequencies and the  $^{15}\text{N}$ - $^1\text{H}$  dipolar couplings.<sup>31</sup> Dynamical information is available from the motional averaging of  $^{15}\text{N}$  chemical shift and  $^{15}\text{H}$ - $^1\text{H}$  dipolar powder patterns and the relaxation analysis of the isotropic  $^{15}\text{N}$  resonances.<sup>32</sup> Samples highly enriched in  $^{15}\text{N}$  are valuable in  $^{13}\text{C}$  solid-state NMR spectroscopy in overcoming the deleterious effects of  $^{14}\text{N}$  dipolar couplings on  $^{13}\text{C}$  spectral resolution<sup>33</sup> and in  $^1\text{H}$

(23) Smith, M. G. *Meth. Enzymol.* **1966**, *12A*, 545–550.

(24) Cross, T. A.; Opella, S. J. *Biochemistry* **1981**, *20*, 290–297.

(25) Opella, S. J.; Frey, M. H. *J. Am. Chem. Soc.* **1979**, *101*, 5854–5856.

(26) Unfortunately there are such large discrepancies among the reported chemical shifts for model compounds in solution<sup>22</sup> that it is not possible at present to draw firm conclusions about the hydrogen bonding or base stacking of DNA on the basis of chemical shift differences. The disagreements in the literature extend to the assignment of the A1 and A3 nitrogen resonances.

(27) Gattegno, D.; Hawkes, G. E.; Randall, E. W. *J. Chem. Soc., Perkin Trans. 2* **1976**, 1527–1531.

(28) Live, D. H.; Wysbrod, H. R.; Fsiehman, A. J.; Agosta, W. C.; Bradley, C. H.; Cowburn, D. *J. Am. Chem. Soc.* **1979**, 474–479.

(29) Kricheldorf, H. R. *Org. Magn. Reson.* **1981**, *15*, 162–177.

(30) The protein resonance assignments are based on the comparison of chemical shifts with model amino acids and peptides. The 50 amino acids' coat protein has 0 Arg, 0 Asn, 1 Gln, 4 Gly, 0 His, 5 Lys, 1 Pro, and 1 Trp among the residues with distinctive  $^{15}\text{N}$  chemical shifts besides the N-terminal amino acid.

(31) DiVerdi, J. A.; Opella, S. J. *J. Am. Chem. Soc.* **1982**, *104*, 1761.

(32) Cross, T. A.; Opella, S. J., unpublished results.

(21) James, T. L.; James, J. L.; Lapidot, A. *J. Am. Chem. Soc.* **1981**, *103*, 6748–6750.

(22) (a) Happe, J. A.; Morales, M. *J. Am. Chem. Soc.* **1966**, *88*, 2077–2078. (b) Markowski, V.; Sullivan, G. R.; Roberts, D. J. *Ibid.* **1977**, *99*, 714–718. (c) Hawkes, G. E.; Randall, E. W.; Hull, W. E. *J. Chem. Soc., Perkin Trans. 2* **1977**, 1268–1275. (d) Buchner, P.; Maurer, W.; Ruterjans, H. *J. Magn. Reson.* **1978**, *29*, 45–63. (e) Poulter, C. D.; Livingston, C. L. *Tetrahedron Lett.* **1979**, 755–758. (f) Dyllick-Brenzinger, C.; Sullivan, G. R.; Pang, P. P.; Roberts, J. D. *Proc. Natl. Acad. Sci. U.S.A.* **1980**, *77*, 5580–5582.

solution NMR spectroscopy in eliminating broadening from  $^{14}\text{N}$  relaxation effects.<sup>34</sup>

**Acknowledgment.** We thank George Furst for helpful discussions. This research is being supported by grants from the National Institute of Health (GM 24266) and the American Cancer Society (NP-225). T.A.C. is supported by a Cell and Molecular Biology Training Grant. S.J.O. is a Fellow of the A. P. Sloan Foundation (1980-1982).

- (33) Hexem, J. G.; Frey, M. H.; Opella, S. J. *J. Am. Chem. Soc.* **1981**, *103*, 224-226.  
 (34) Madison, V.; Kopple, K. D. *J. Am. Chem. Soc.* **1980**, *102*, 4855-4863.  
 (35) Dixon, W. T. *J. Magn. Reson.* **1981**, *44*, 220-223.

## N-H Bond Lengths in DNA

J. A. DiVerdi and S. J. Opella\*

*Department of Chemistry, University of Pennsylvania  
 Philadelphia, Pennsylvania 19104*

*Received November 5, 1981*

Because of its central role in biology, the structure of DNA is of substantial interest and has been the subject of numerous investigations. X-ray diffraction studies of oriented polymer fibers<sup>1,2</sup> and crystals of oligonucleotides<sup>3</sup> have described the conformations of DNA in considerable detail based on the positions of the C, N, O, and P atoms. In spite of the importance of interstrand hydrogen bonds to the structure and biological roles of DNA, little is known about the locations of the hydrogens between the base pairs because of the limitations of X-ray diffraction. Both X-ray<sup>4</sup> and neutron<sup>5</sup> diffraction have been used to measure N-H bond lengths of hydrogen-bond donors; however, the results are from crystals of methylated bases participating in Hoogsteen rather than Watson-Crick base pairs.

NMR spectroscopy is well suited for structure determinations, especially in locating the positions of protons, through the spatial dependence of internuclear dipole-dipole couplings.<sup>6</sup> The large number of dipolar interactions in complex chemical systems result in severe spectral overlap among sites and couplings. Separated local field spectroscopy uses chemical shift positions to distinguish among individual sites and selective averaging techniques to measure the heteronuclear dipolar couplings at those sites.<sup>7</sup> The dipolar interactions between carbons and protons have been characterized with this approach in single crystals,<sup>8</sup> oriented fibers,<sup>9</sup> and powder samples.<sup>10,11</sup>

Uniformly  $^{15}\text{N}$  labeled DNA gives solid-state NMR spectra with resolved resonances for nearly all nitrogen sites;<sup>12</sup> in particular, both the hydrogen-bond donor and acceptor nitrogens of the adenine-thymine (AT) and guanine-cytosine (GC) base pairs can be distinguished. By determination of the size of the  $^{15}\text{N}$ - $^1\text{H}$

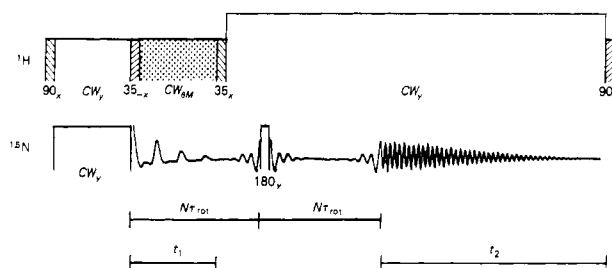


**Figure 1.** Schematic outline of the pulse sequence used for magic-angle sample spinning separated local field spectroscopy.  $^1\text{H}$  represents the procedure applied at the proton resonance frequency:  $P_x$  are pulses of rotation angle  $P$  with relative phases  $x = 0^\circ$  or  $-x = 180^\circ$ ;  $\text{CW}_y$  is continuous irradiation on resonance of phase  $y = 90^\circ$  relative to  $x$ ;  $\text{CW}_{MM}$  is continuous irradiation off-resonance for magic-angle decoupling as described by Lee and Goldburg.<sup>14</sup>  $^{15}\text{N}$  represents the procedures applied at the nitrogen resonance frequency: the continuous on-resonance mixing irradiation (CW) and the  $180^\circ$  pulse have the same phase. The free-induction decays are actual experimental data from a molecule with a single nitrogen drawn to scale, except for the length of interval  $t_2$ .  $\tau_{\text{rot}}$  is the time for one sample rotation and  $N$  is an integer.  $t_1$  and  $t_2$  are the two sampling intervals.

dipolar couplings of these sites and hence the bond lengths, the hydrogen bonds can be fully characterized as long as they are assumed to be linear. Because magic-angle sample spinning is used to average the chemical shift to its isotropic value in the unoriented polymer samples, the  $^{15}\text{N}$ - $^1\text{H}$  dipolar spectra are in the form of Pake powder patterns modulated by the spinning frequency and are observed as dipolar sidebands.<sup>11</sup>

The experimental procedure for separate local field spectroscopy with magic-angle sample spinning is outlined in Figure 1. Initial  $^1\text{H}$  magnetization is developed in the static magnetic field and then spin locked on resonance with a  $90^\circ$  pulse followed by continuous irradiation shifted in phase by  $90^\circ$ . The  $^{15}\text{N}$  magnetization is prepared by simultaneously applying a mixing pulse under Hartmann-Hahn matching conditions.<sup>13</sup> The initial  $^{15}\text{N}$  magnetization is allowed to precess for the time interval  $t_1$ , which is systematically incremented in the course of the experiments. During the  $t_1$  interval, spin diffusion among the protons is suppressed by decoupling the  $^1\text{H}$ - $^1\text{H}$  dipolar interactions with a radiofrequency field applied off-resonance, such that the effective field in the rotating frame points along a direction inclined at the magic angle with respect to the static magnetic field.<sup>14</sup> This magic-angle decoupling scales the  $^{15}\text{N}$ - $^1\text{H}$  dipolar coupling by  $3^{-1/2}$ . The dipolar precession is monitored during time interval  $t_2$ , when fully  $^1\text{H}$  decoupled  $^{15}\text{N}$  isotropic chemical shift free-induction decays are recorded. Additional  $^1\text{H}$  pulses are inserted in the sequence to preserve coherence of the  $^1\text{H}$  magnetization in the rotating frame and to flip back any  $^1\text{H}$  magnetization not transferred to the  $^{15}\text{N}$  spins or lost to  $T_{1\rho}$  processes to the laboratory frame for optimal sensitivity of the experiment. The  $^{15}\text{N}$   $180^\circ$  pulse refocuses the chemical shift precession, so that pure  $^{15}\text{N}$ - $^1\text{H}$  dipolar spectra are obtained. The entire procedure is synchronized with the sample rotation, such that the  $^{15}\text{N}$   $180^\circ$  pulse and the start of interval  $t_2$  are integral multiples of the sample rotation period.

The spectra in Figure 2 are obtained by Fourier transformation of free-induction decays associated with time intervals  $t_1$  (dipolar couplings in kHz) and  $t_2$  (chemical shift in ppm). The isotropic chemical shift spectra are of hydrated B form DNA<sup>15</sup> (Figure 2A) and low-humidity DNA<sup>16</sup> (Figure 2B). The contour plots in Figure 2C represent the intensities of the dipolar sidebands aligned with the chemical shift positions of Figure 2B. The qualitative correlation of chemical shift with the magnitude of the dipolar

- (1) Watson, J. D.; Crick, F. H. C. *Nature (London)* **1953**, *171*, 737-738.  
 (2) Arnott, S. *Prog. Biophys. Mol. Biol.* **1970**, *21*, 267-319.  
 (3) (a) Wang, A. H.-J.; Quigley, G. J.; Kolpak, F. J.; Crawford, J. L.; van Boom, J. H.; van der Morel, G.; Rich, A. *Nature (London)* **1979**, *282*, 680-686. (b) Wing, R.; Drew, H.; Takano, T.; Broka, C.; Tanaka, S.; Itakura, K.; Dickerson, R. *Ibid.* **1980**, *287*, 755-758.  
 (4) (a) Hoogsteen, K. *Acta Crystallogr.* **1963**, *16*, 28-38. (b) Hoogsteen, K. *Ibid.* **1963**, *16*, 907-916.  
 (5) (a) Frey, M. N.; Koetzke, T. F.; Lehmann, M. S.; Hamilton, W. C. *J. Chem. Phys.* **1973**, *59*, 915-924. (b) Kvick, A.; Koetzke, T. F.; Thomas, R. *Ibid.* **1974**, *61*, 2711-2719.  
 (6) Pake, G. J. *J. Chem. Phys.* **1948**, *16*, 327-336.  
 (7) Waugh, J. S. *Proc. Natl. Acad. Sci. U.S.A.* **1976**, *73*, 1394-1397.  
 (8) (a) Hester, R. K.; Ackerman, J. L.; Neff, B. L.; Waugh, J. S. *Phys. Rev. Lett.* **1976**, *36*, 1081-1083. (b) Rybaczewski, E. F.; Neff, B. L.; Waugh, J. S.; Sherfinski, J. S. *J. Chem. Phys.* **1977**, *67*, 1231-1236. (c) Stoll, M. E.; Vega, A. J.; Vaughan, R. W. *Ibid.* **1976**, *65*, 4808-4809. (d) Stoll, M. E.; Vega, A. J.; Vaughan, R. W. *Ibid.* **1976**, *65*, 4093-4098.  
 (9) Opella, S. J.; Waugh, J. S. *J. Chem. Phys.* **1977**, *66*, 4919-4924.  
 (10) Linder, M.; Hohener, A.; Ernst, R. R. *J. Chem. Phys.* **1980**, *73*, 4959-4970.  
 (11) Munowitz, M. G.; Griffin, R. G.; Bodenhausen, G.; Huang, T. H. *J. Am. Chem. Soc.* **1981**, *103*, 2529-2533.  
 (12) Cross, T. A.; DiVerdi, J. A.; Opella, S. J. *J. Am. Chem. Soc.* **1982**, *104*, 1759.

- (13) Hartmann, S. R.; Hahn, E. L. *Phys. Rev.* **1962**, *128*, 2042-2053.  
 (14) Lee, M.; Goldburg, W. I. *Phys. Rev.* **1965**, *140*, 1261-1271.  
 (15) Langridge, R.; Marvin, D. A.; Seeds, W. E.; Wilson, H. R.; Hooper, C. W.; Wilkins, M. H. F. *J. Mol. Biol.* **1960**, *2*, 38-64.  
 (16) Franklin, R. E.; Gosling, R. G. *Acta Crystallogr.* **1953**, *6*, 673-677.  
 (17) Arnott, S.; Dover, S. D.; Wonacott, A. J. *Acta Crystallogr.* **1969**, *B25*, 2192-2206.